






Cross-modal Fundus Image Registration under Large FoV Disparity

Hongyang Li¹, Junyi Tao¹, Qijie Wei¹, Ningzhi Yang¹, Meng Wang²,
Weihong Yu², and Xirong Li^{*1}

¹ Renmin University of China, Beijing, China

² Peking Union Medical College Hospital, Beijing, China

<https://github.com/ruc-aimc-lab/care>

Abstract. Previous work on cross-modal fundus image registration (CMFIR) assumes small cross-modal Field-of-View (FoV) disparity. By contrast, this paper is targeted at a more challenging scenario with large FoV disparity, to which directly applying current methods fails. We propose Crop and Alignment for cross-modal fundus image Registration(**CARE**), a very simple yet effective method. Specifically, given an OCTA with smaller FoV as a source image and a wide-field color fundus photograph (wfCFP) as a target image, our *Crop* operation exploits the physiological structure of the retina to crop from the target image a sub-image with its FoV roughly aligned with that of the source. This operation allows us to re-purpose the previous *small-FoV-disparity* oriented methods for subsequent image registration. Moreover, we improve spatial transformation by a double-fitting based *Alignment* module that utilizes the classical RANSAC algorithm and polynomial-based coordinate fitting in a sequential manner. Extensive experiments on a newly developed test set of 60 OCTA-wfCFP pairs verify the viability of **CARE** for CMFIR.

Keywords: CMFIR · Large FoV disparity · Double fitting

1 Introduction

This paper aims for *cross-modal* fundus image registration (CMFIR) under large Field-of-View (FoV) disparity, an emerging challenge arising with the development of fundus imaging techniques. More and more retinal lesions can nowadays be visualized in a *noninvasive* manner. Consider for instance non-perfusion area (NPA), a crucial feature of microvascular injury. Previously, NPA had to be identified through invasive fluorescein angiography (FA), see Fig. 1a. It can now be identified via noninvasive OCT angiography (OCTA) [3]. Registering an OCTA image to a wide-field color fundus photograph (wfCFP) of the same eye produces a composite image with enhanced clinical value, see Fig. 1b.

(Cross-modal) Fundus image registration has been actively studied [2, 9, 17–19, 22, 23], with feature (or keypoint) based methods as the mainstream solution. In order to register a specific source image *w.r.t.* a given target image, a

* Corresponding author: Xirong Li (xirong@ruc.edu.cn)

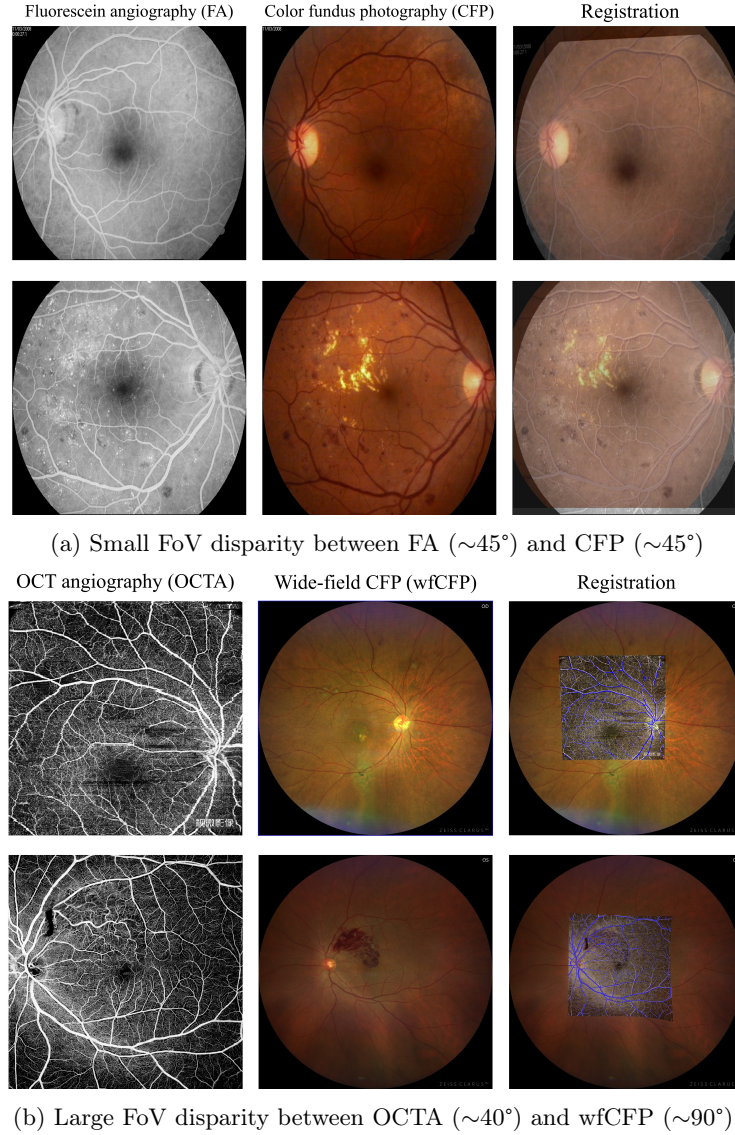


Fig. 1: **Cross-modal fundus image registration** (CM-FIR) under (a) small and (b) large FoV disparity. While existing works focus on the former, this paper tackles the latter.

feature-based method typically performs feature or keypoint detection, followed by feature matching to find a correspondence between a set of keypoints. Based on the correspondence, a specific spatial transforming function, with homography as a common choice, is then fitted. Much progress has been made, with generic

feature detectors [4, 11] replaced by fundus-specific alternatives such as SuperRetina [9] and SuperJunction [18], the brute-force matcher replaced by learnable alternatives like SuperGlue [15], *etc.* Existing methods typically assume small FoV disparity between the source and target images, see Fig. 1a. Under large cross-modal FoV disparity, as in the case of OCTA-to-wfCFP, both the feature matching and coordinate fitting processes become erroneous. As exemplified in Fig. 2, simply re-purposing the SOTA methods [9, 17, 18] for the new task fails.

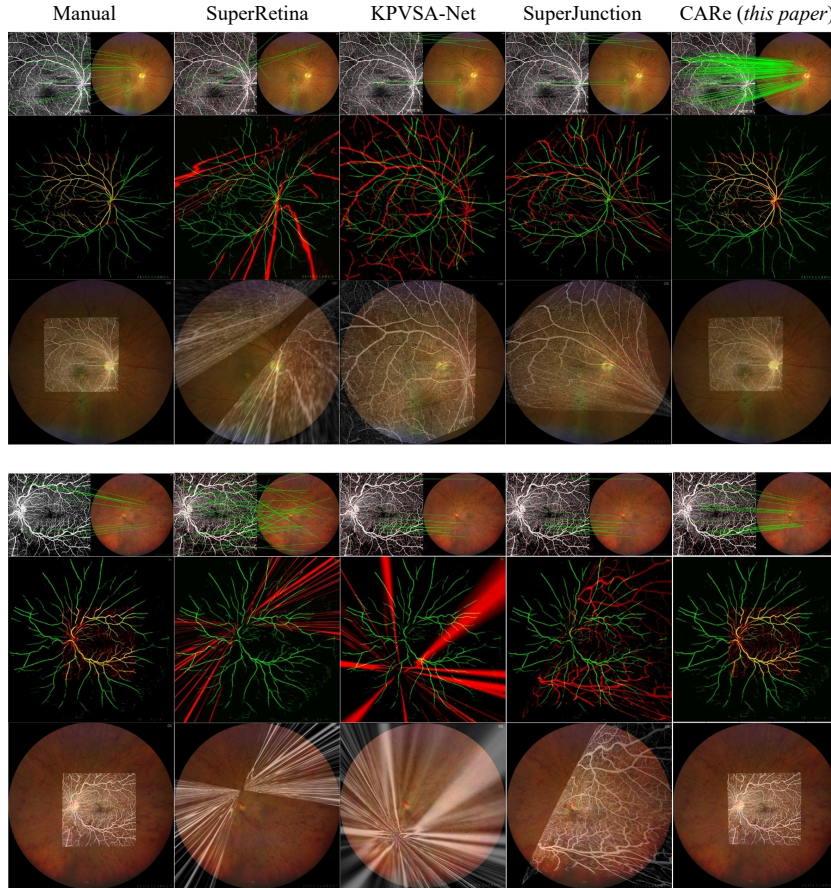


Fig. 2: **Visualization of registering a specific OCTA image to a wfCFP image of the same eye.** Vessels in red are from the OCTA, while vessels in green are from the wfCFP. The cross-modal aligned vessels are highlighted in yellow. More yellows mean better alignments. Simply re-training current *small-FoV-disparity* oriented methods (SuperRetina [9], KPVSA-Net [17] and SuperJunction [18]) does not work. Best viewed digitally.

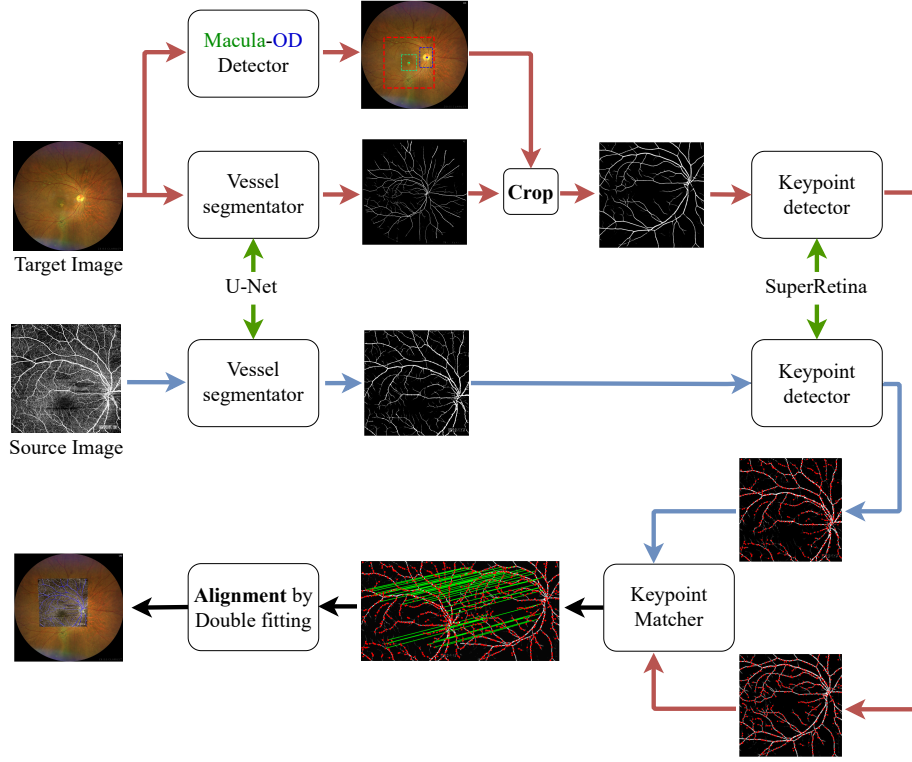


Fig. 3: **Conceptual diagram of the proposed CARE method.** In order to tackle CM-FIR under large FoV disparity, our method contains *task-specific* designs as follows: i) U-Net based *unified* vessel segmentation that converts cross-modal fundus images (OCTA and wCFP) to a unified vessel map representation, ii) *Crop* for coarse FoV alignment achieved by cropping a sub-image from the target image based on jointly detected macula and optic disc (OD), iii) an improved training procedure of SuperRetina for better keypoint matching, and iv) *Align* for source-to-target coordinate transformation by *double fitting*, involving a novel cascaded use of RANSAC and polynomial-based coordinate fitting.

To attack the new challenge, we propose Crop and Alignment for cross-modal fundus image Registration (**CARE**), see Fig. 3. Our idea is very simple. Noting the large FoV disparity as the main obstacle, we propose a **Crop** operation to achieve a rough cross-modal FoV alignment at the first place. Despite its simplicity, such an operation allows us to re-purpose the previous *small-FoV-disparity* oriented methods for subsequent fundus image registration. Furthermore, we improve coordinate transformation by a double-fitting that makes a cascaded use of the classical RANSAC algorithm and polynomial-based coordinate fitting. To sum up, our major contributions are as follows.

- To the best of our knowledge, we are the first to tackle CMFIR under large FoV disparity. To that end, we build **OCTA60**, a test set of 60 OCT-wfCFP pairs, collected from Outpatient Clinic with images showing varied fundus conditions of real-world patients.
- We propose **CARe**, a simple yet effective method that uses a **Crop** operation, which exploits the physiological structure of wfCFP, to simplify the registration process and an **Alignment** module to improve the registration accuracy. Moreover, we improve the training procedure of SuperRetina for better keypoint matching in the cross-modal scenario.
- Extensive experiments on the **OCTA60** test set verify the superiority of the proposed method over multiple strong baselines [9, 17, 18] re-purposed for the new task.

2 Related Work

2.1 Methods for CMFIR

Current methods for CMFIR are feature-based, extracting discriminative features either from fundus images [17, 22] or from their vascular maps [19, 23], followed by feature matching to establish spatial correspondences between given image pairs. As vascular maps naturally provide a unified representation of cross-modal fundus images, we follow [19, 23], extracting features from the vascular maps. However, different from [19, 23] which uses SuperPoint [4], a generic feature detector and descriptor, we adopt SuperRetina [9] that is specifically developed for fundus image matching. Moreover, we go one step further by addressing CMFIR under large FoV disparity, a new and more challenging task not considered by the previous works.

2.2 Datasets for CMFIR

To the best of our knowledge, FA-CFP [6] is the only public dataset³, including 59 pairs of CFP and FA images with small cross-modal FoV disparity, see Fig. 1a. As the dataset has no annotation *w.r.t.* keypoint correspondence, the registration accuracy of a specific method is indirectly measured by the Dice similarity between the vessel maps of a target image and a registered source image. Our proposed **OCTA60** test set is targeted at the more challenging setting of large cross-modal FoV disparity. Moreover, we provide manually annotated keypoint correspondences per pair for a more comprehensive evaluation.

3 Proposed CARe Method

Given a pair of cross-modal fundus images captured from the same eye, the goal of CMFIR is to spatially transform the fundus image of smaller FoV, *a.k.a.*

³ <https://misp.mui.ac.ir/en/node/1498>

the source image, to align with the other image of larger FoV, *a.k.a.* the target image. More formally, we aim to build a source-to-target coordinate transforming function F that for each pixel positioned by (u, v) in the source image, its counterpart (x, y) in the target image can be well approximated by $F(u, v)$. Our method is feature-based, with F developed based on a correspondence between a set of m keypoints $P = \{((u_i, v_i), (x_i, y_i))\}_{i=1}^m$ obtained by keypoint detection and matching. For keypoint detection and description in a cross-modal manner, we adopt a unified vessel segmentor to convert the cross-modal images to vascular maps. To handle the large cross-modal FoV disparity, we propose a simple yet effective **Crop** operation, exploiting the physiological structure of the retina to crop from the target image a region roughly aligned with the source image. Feature matching is then performed on the vessel maps of the source image and the cropped target image. Lastly, for accurate source-to-target coordinate transformation, a double-fitting based **Alignment** module is developed.

3.1 Unified Vessel Segmentation

In order to convert the fundus images of distinct modalities to a unified vessel map representation, we train a U-Net [14] based vessel segmentation network. Following [20], our training data is a joint set of public datasets of varied modalities including FIVES for CFP [7], ROSSA for OCTA [12], IOSTAR for scanning laser ophthalmoscopy [1], PRIME-FP20 for ultra-wide-field fundus imaging [5] and VAMPIRE for FA [13]. We empirically find that such a simple solution is sufficient to extract good-quality vessel maps, see Fig. 4, for keypoint detection and description. An important merit of using the unified vessel segmentor is that our method will be directly applicable to varied modality combinations such as OCTA-CFP and FA-CFP, with no need of combination-specific re-training.

3.2 Crop for Coarse FoV Alignment

As shown in Fig. 1b, the source image in this study was obtained by OCTA, which visualizes detailed microvasculature in the macula. Hence, for a coarse FoV alignment between the source and target images, we propose to crop the macular area of the target image. As the macula and the optic disc (OD) are spatially correlated, previous work suggests that jointly detecting the two regions of interest (ROIs) is more accurate and reliable than detecting them alone [21]. In that regard, we train RetinaNet [8], a widely used one-stage object detection network, on 117 labeled examples. Evaluation on a hold-out test set of 25 images shows that RetinaNet detects both ROIs with mean IoU of around 0.75, sufficiently accurate for our purpose. Based on the auto-located macula and OD, we crop an area roughly corresponding to the posterior pole of the retina. As shown in Fig. 3, the cropped region is a square centered on the macula, with its side length dynamically determined as twice the distance from the macular center to the outer edge of the detected optic-disc region. As shown in Fig. 4, compared to the original target images, the FoVs of the cropped sub-images are much more close to those of the source images.

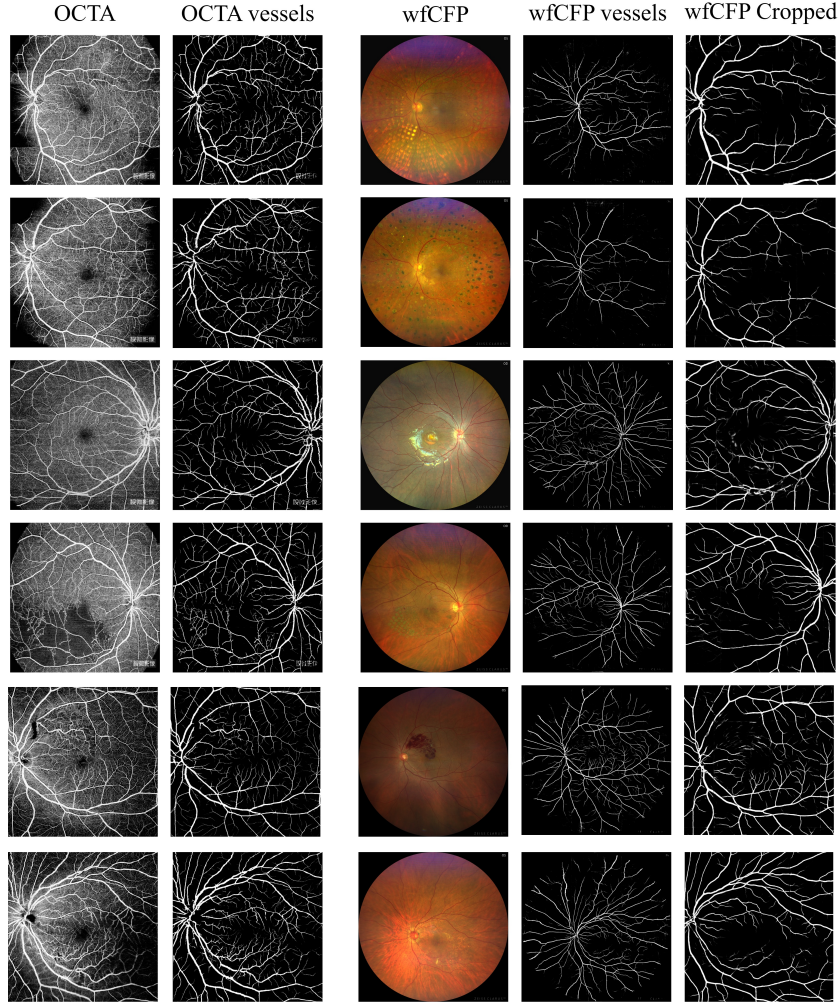


Fig. 4: Vessel segmentation and cropping results. Best viewed digitally.

3.3 Improved SuperRetina for Keypoint Detection and Matching

We adopt SuperRetina [9], an end-to-end network that detects keypoints, *i.e.*, crossovers and bifurcations on the vascular tree, and generates their descriptors simultaneously from a given fundus image. Note that SuperRetina, originally developed for uni-modal image registration, takes CFP images as its input. So for input adaptation, we re-train the network on a set of 44 wfCFP vessel maps with manually labeled keypoints. While in theory we shall collect paired images with known spatial correspondence for training, such paired samples are practically generated by applying controlled homography per training image [4]. As

such, SuperRetina can be trained in a semi-supervised manner. Given keypoints detected from the vessel maps of the source image and the cropped target image, respectively, we use the classical OpenCV Brute-Force matcher (BFMatcher) to obtain the matched keypoint set P .

It is worth pointing out that due to their distinct imaging techniques, OCTA images reveal richer capillary structures with greater details than their wfCFP counterparts, see Fig. 4. Recall that SuperRetina is trained exclusively on wfCFP. Such a divergence introduces a domain gap between keypoint descriptors (or features) learned in the training stage and their counterparts used in the inference stage, and thus makes P suboptimal.

To bridge the domain gap, we simulate the cross-modal vessel divergence by performing a classical **opening** operation (an erosion followed by a dilation) on one image per training pair. As a consequence, the processed image loses fine-grained vascular details to some extent. Training with such asymmetrically manipulated image pairs allows SuperRetina to better align local features between OCTA and wfCFP images.

3.4 Fine-grained Alignment by Double Fitting

For coordinate transformation, previous work typically makes the planar assumption about the fundus images [9, 19, 23], hence fitting F by RANSAC-based homography estimation. However, this assumption becomes questionable for large FoV and high-resolution images, *e.g.*, 1000×1000 in this work. RANSAC is reliable yet less accurate. The retinal images are two-dimensional projections of the three-dimensional eyeball, making them subject to nonlinear transformations. In contrast, the homography transformation computed by RANSAC is a linear transformation, which can therefore lead to a loss of accuracy. Alternatively, recent work [18] employs polynomial fitting [16]. Although accurate, we empirically find that such a fitting strategy is rather sensitive to outliers.

In order to leverage the reliability of RANSAC and the accuracy of polynomial fitting, we propose a very simple yet effective double-fitting strategy. The strategy, dubbed **RAN-Poly**, first uses RANSAC to remove outliers from P , and then fits the following n -degree polynomial functions:

$$\begin{cases} x = \sum_{i+j \leq n} a_{ij} u^i v^j \\ y = \sum_{i+j \leq n} b_{ij} u^i v^j, \end{cases} \quad (1)$$

where $a_{i,j}$ and $b_{i,j}$ are polynomial coefficients optimized by the least square method. A larger n means a stronger fitting capability, yet with an increased risk of over-fitting. In the context of uni-modal fundus image registration, Wang *et al.* [18] empirically show that a quadratic polynomial works the best. We follow their recommendation, using $n = 2$ in this work. The validity of this choice is also confirmed by our ablation study. The RAN-Poly double fitting strategy allows us to largely relax the planar assumption, and thus obtain more accurate coordinate transformation.

RAN-Poly is conceptually connected to the bias-variance tradeoff. Polynomial fitting, as its polynomial degree increases, becomes more flexible to fit a training dataset with lower bias, yet there will be greater variance in the model’s estimated parameters. By contrast, RANSAC-based homography estimation, with its planar assumption and the fixed number of trainable parameters, has smaller variance yet greater bias. By combining RANSAC and polynomial fitting, RAN-Poly achieves a good bias-variance tradeoff.

4 Experiments

4.1 Experimental Setup

Test data. We collect 60 pairs of OCTA and wfCFP images from 60 distinct patients at the outpatient clinic of the Department of Ophthalmology in a state hospital between Feb. 2023 and Dec. 2023. In particular, OCTA projections of the superficial vascular plexus (SVP) layer were acquired by a $12\text{mm} \times 12\text{mm}$ scan centered on the macula using a SVision VG200 OCT, while wfCFPs were acquired using a ZEISS CLARUS 500 fundus camera. Each image pair has at least 10 manually labeled keypoint correspondences as ground truth. All images are resized to 1000×1000 in advance. They shows varied fundus conditions of real-world patients, challenging the robustness of the proposed method. This study is complied with the Declaration of Helsinki. We term the test set **OCTA60**.

Performance metrics. Following [9], we report the failed / inaccurate / acceptable rate. A registration is considered acceptable if the median Euclidean error (MEE) and the maximum Euclidean error (MAE) between the mapped keypoints and the ground truth are less than 20 and 50 pixels, respectively. We also report AUC with the MEE threshold ranging from 1 to 25. For a more in-depth analysis, we report the average number of keypoint matches per OCTA-wfCFP pair. A match is considered *acceptable* if the matched keypoint is within 20 pixels to the corresponding reference point. In addition, we report soft Dice Coefficient Dice_s [22], reflecting the overlap between the vessel maps of the target image and the registered source image.

Implementation. Training details of the networks used for vessel segmentation, macula / OD detection and keypoint detection are listed in Table 1. All experiments were conducted on an NVIDIA 2080ti GPU with the following software environment: Ubuntu 18.04, CUDA 11.7 and PyTorch 1.21.

Baselines. We compare with the following SOTA feature-based methods, *i.e.*, SuperRetina [9], KPVSA-Net [17] and SuperJunction [18]. See Table 2 for their choices of keypoint matcher and transformation fitting. For a fair comparison we re-train their modules on our training data whenever applicable. In particular, the same vessel segmentor and keypoint detector are used. Comparison with detector-free methods [10] is reserved for future work.

4.2 Comparison with Baseline Methods

Results on OCTA60. As shown in Table 2 and Fig. 2, all the baselines fail to generate acceptable registration results, showing their ineffectiveness in handling

Table 1: **Training details of the three deep networks used in the proposed method:** U-Net for vessel segmentation, Retina-Net for macula / OD detection and SuperRetina for feature detection and description.

Network	Optimizer	Epochs	Learning rate	Batch size
U-Net	SGD	100	1e-3	5
RetinaNet	Adam	150	1e-5	1
SuperRetina	Adam	150	1e-3	4

the large inter-modal FoV disparity. Note that SuperGlue tends to yield more matches, albeit incorrect, than BFMatcher. Therefore, the failed rate of [17, 18], which use SuperGlue, is much lower than that of [9] which uses BFMatcher. Our method clearly outperforms the baselines in terms of all performance metrics.

Table 2: **Results on OCTA60.** DLT: Direct linear transformation. Poly: Polynomial fitting. RAN: RANSAC.

Method	Matcher	Fitting	Failed[%]↓	Inaccurate[%]↓	Acceptable[%]↑	AUC↑	Dice _s ↑
SuperRetina [9]	BFMatcher	RANSAC	78.33	20.00	1.67	0.016	0.082
KPVSA-Net [17]	SuperGlue	DLT	8.33	91.67	0	0	0.077
SuperJunction [18]	SuperGlue	Poly	23.33	76.67	0	0	0.076
CARe		RAN-Poly	0.00	1.67	98.33	0.920	0.295
<i>w/o Crop</i>		RAN-Poly	55.00	43.33	1.67	0.019	0.051
<i>w/o Opening</i>	BFMatcher	RAN-Poly	3.33	3.33	93.33	0.896	0.282
<i>w/o RANSAC</i>		Poly	0.00	31.67	68.33	0.596	0.219
<i>w/o Poly</i>		RANSAC	0.00	3.33	96.67	0.912	0.289

For a better understanding, for each method, we report in Table 3 the average number of keypoint matches per OCTA-wfCFP pair. A match is considered *acceptable* if the matched keypoint is within 20 pixels to the corresponding reference point. Facing large cross-modal FoV disparity, the existing methods have much fewer matches with much lower acceptable match rate. Hence, the fact that existing methods struggle with large FoV disparity can be largely attributed to their incapability to find sufficient and acceptable keypoint matches for the subsequent transformation fitting.

Results on FA-CFP. To check how our **Alignment** module⁴ works in the traditional setting (of small cross-modal FoV disparity), we evaluate the module on the public FA-CFP dataset [6]. We report Dice_s only, as the FA-CFP dataset has no keypoint correspondence, which makes it unfeasible to calculate metrics

⁴ Here we omit the **Crop** operation, which makes no practical difference for CFP with relatively small FoV as in the FA-CFP dataset.

Table 3: **Averaged number of keypoint matches per OCTA-wfCFP pair.**

Method	#Matches \uparrow	Acceptable-match rate \uparrow
SuperRetina [9]	20.8	0.152
KPVSA-Net [17]	35.3	0.008
SuperJunction [18]	35.3	0.008
CARe	149.46	0.978

Table 4: **Results on the FA-CFP testset.**

Method	Dice _s
SuperRetina [9]	0.530
KPVSA-Net [17]	0.319
SuperJunction [18]	0.243
CARe	0.556

other than Dice_s. As Table 4 shows, the **Alignment** module alone again surpasses the baseline methods even when the cross-modal FoV disparity is relatively small.

4.3 Ablation Study

The importance of Crop. As Table 2 shows, using the **Crop** operation or not has a decisive impact on the performance.

Whether Crop helps the baselines? The answer is yes, see Table 5, with the largest improvement made for [9]. Still, our method is better than the much improved baseline, showing the superiority of RAN-Poly to RANSAC.

Table 5: **Performance of the baseline methods with (+) and without (-) our Crop operation.** Test set: **OCTA60**.

Method	Crop?	Acceptable[%] \uparrow	AUC \uparrow	Dice _s \uparrow
SuperRetina [9]	-	0	0	0.081
	+	91.67	0.861	0.269
KPVSA-Net [17]	-	0	0	0.078
	+	60.00	0.587	0.140
SuperJunction [18]	-	0	0	0.079
	+	36.67	0.248	0.116

Impact of the opening operation. Without the opening operation, AUC drops from 0.9833 to 0.9333 (Table 2). Hence, adding the operation improves SuperRetina-based keypoint matching.

The necessity of RAN-Poly. Replacing RAN-Poly either by polynomial fitting or by RANSAC causes performance degeneration, see the last two rows in Table 2. The necessity of our proposed RAN-Poly strategy is thus justified.

Choice of the polynomial degree. Fig. 5 shows the performance curve of the proposed method with different degrees of polynomial functions. The second-degree polynomial strikes the best balance between improving the fitting accuracy and reducing the risk of over-fitting.

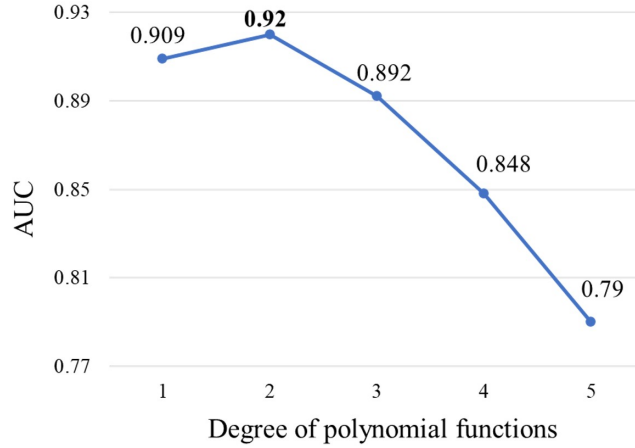


Fig. 5: Performance of CARE with different degrees of polynomial functions used for polynomial fitting. The quadratic polynomial is the best.

5 Conclusions

This paper tackles an emerging challenge of cross-modal fundus image registration (CMFIR) with large FoV disparity. Experiments on the newly developed **OCTA60** test set allow us to draw conclusions as follows. Directly re-purposing existing small-FoV-disparity oriented methods does not work. Coarse FoV alignment by the proposed **Crop** operation is crucial. The SOTA methods can be much improved by this operation, though still less effective than the proposed **CARE** method. For the estimation of the spatial transforming function, the double-fitting strategy, *i.e.*, RAN-Poly, is better than using RANSAC or polynomial fitting alone. While targeted at large cross-modal FoV disparity, our method also works well in the conventional small-FoV-disparity scenario. With **CARE** and **OCTA60**, we establish a new baseline for CMFIR.

Acknowledgments. This research was supported by National Natural Science Foundation of China (62576348, 62172420) and Beijing Natural Science Foundation (L254039).

References

1. Abbasi-Sureshjani, S., Smit-Ockeloen, I., Zhang, J., Ter Haar Romeny, B.: Biologically-inspired supervised vasculature segmentation in SLO retinal fundus images. In: ICIAR (2015)
2. Chen, J., Tian, J., Lee, N., Zheng, J., Smith, R., Laine, A.: A partial intensity invariant feature descriptor for multimodal retinal image registration. *IEEE Transactions on Biomedical Engineering* **57**(7), 1707–1718 (2010)
3. De Carlo, T., Romano, A., Waheed, N., Duker, J.: A review of optical coherence tomography angiography (OCTA). *International Journal of Retina and Vitreous* **1**, 1–15 (2015)
4. DeTone, D., Malisiewicz, T., Rabinovich, A.: SuperPoint: Self-supervised interest point detection and description. In: CVPR workshops (2018)
5. Ding, L., Kuriyan, A., Ramchandran, R., Wykoff, C., Sharma, G.: Weakly-supervised vessel detection in ultra-widefield fundus photography via iterative multi-modal registration and learning. *IEEE Transactions on Medical Imaging* **40**(10), 2748–2758 (2020)
6. Hajeb Mohammad Alipour, S., Rabbani, H., Akhlaghi, M.: Diabetic retinopathy grading by digital curvelet transform. *Computational and Mathematical Methods in Medicine* **2012**(1), 761901 (2012)
7. Jin, K., Huang, X., Zhou, J., Li, Y., Yan, Y., Sun, Y., Zhang, Q., Wang, Y., Ye, J.: FIVES: A fundus image dataset for artificial intelligence based vessel segmentation. *Scientific Data* **9**(1), 475 (2022)
8. Lin, T., Goyal, P., Girshick, R., He, K., Dollár, P.: Focal loss for dense object detection. In: ICCV (2017)
9. Liu, J., Li, X., Wei, Q., Xu, J., Ding, D.: Semi-supervised keypoint detector and descriptor for retinal image matching. In: ECCV (2022)
10. Liu, J., Li, X.: Geometrized transformer for self-supervised homography estimation. In: ICCV (2023)
11. Lowe, D.G.: Distinctive image features from scale-invariant keypoints. *International Journal of Computer Vision* **60**, 91–110 (2004)
12. Ning, H., Wang, C., Chen, X., Li, S.: An accurate and efficient neural network for OCTA vessel segmentation and a new dataset. In: ICASSP (2024)
13. Perez-Rovira, A., Zutis, K., Hubschman, J., Trucco, E.: Improving vessel segmentation in ultra-wide field-of-view retinal fluorescein angiograms. In: EMBC (2011)
14. Ronneberger, O., Fischer, F., Brox, T.: U-Net: Convolutional networks for biomedical image segmentation. In: MICCAI (2015)
15. Sarlin, P., DeTone, D., Malisiewicz, T., Rabinovich, A.: SuperGlue: Learning feature matching with graph neural networks. In: CVPR (2020)
16. Sharma, L., Sharma, J., Anand, D., Sharma, S.: An adaptive window based polynomial fitting approach for pixel matching in stereo images. In: ICICCT (2018)
17. Sindel, A., Hohberger, B., Maier, A., Christlein, V.: Multi-modal retinal image registration using a keypoint-based vessel structure aligning network. In: MICCAI (2022)
18. Wang, Y., Wang, X., Gu, Z., Liu, W., Ng, W., Huang, W., Cheng, J.: SuperJunction: Learning-based junction detection for retinal image registration. In: AAAI (2024)
19. Wang, Y., Zhang, J., An, C., Cavichini, M., Jhingan, M., Amador-Patarroyo, M., Long, C., Bartsch, D., Freeman, W., Nguyen, T.: A segmentation based robust deep learning framework for multimodal retinal image registration. In: ICASSP (2020)

20. Wei, Q., Yu, W., Li, X.: Convolutional prompting for broad-domain retinal vessel segmentation. In: ICASSP (2025)
21. Yang, Z., Li, X., He, X., Ding, D., Wang, Y., Dai, F., Jin, X.: Joint localization of optic disc and fovea in ultra-widefield fundus images. In: MLMI (2019)
22. Zhang, J., An, C., Dai, J., Amador, M., Bartsch, D., Borooah, S., Freeman, W., Nguyen, T.: Joint vessel segmentation and deformable registration on multi-modal retinal images based on style transfer. In: ICIP (2019)
23. Zhang, J., Wang, Y., Dai, J., Cavichini, M., Bartsch, D., Freeman, W., Nguyen, T., An, C.: Two-step registration on multi-modal retinal images via deep neural networks. *IEEE Transactions on Image Processing* **31**, 823–838 (2021)